EXPERIMENTAL ACTIVE AND PASSIVE DOSIMETRY SYSTEMS FOR THE NASA SKYLAB PROGRAM

CAPT MARION F. SCHNEIDER, JOSEPH F. JANNI, AND GLENN C. AINSWORTH

Technology Division
Air Force Weapons Laboratory

Active and passive dosimetry instrumentation to measure absorbed dose, charged particle spectra, and linear energy transfer spectra inside the command module and orbital workshop on the NASA Skylab Program in 1972 have been developed and tested.

The active dosimetry system consists of one integral unit employing both a tissue equivalent ionization chamber and silicon solid state detectors. The instrument measures dose rates from 0.2 millirad/hour to 25 rads/hour, linear energy transfer spectra from 2.8 to 42.4 Kev/micron, and the proton and alpha particle energy spectra from 0.5 to 75 Mev. The active dosimeter is equipped with a portable radiation sensor for use in astronaut on-body and spacecraft shielding surveys during passage of the Skylab through significant space radiations. Data are transmitted in real time or are recorded by on-board spacecraft tape recorder for rapid evaluation of the radiation levels.

The passive dosimetry systems consist of twelve (12) hard-mounted assemblies, each containing a variety of passive radiation sensors which are recoverable at the end of the mission for analysis. The passive dosimeters consist of calcium and lithium fluoride thermoluminescent dosimeters, special discharge ionization chambers, activation foils, Ilford G.5 and K.2 nuclear emulsions and plastic heavy particle track dosimeters. The passive dosimeters record the total mission dose from 5 millirads to 5000 rads and the linear energy transfer spectra from 0.20 to >85 Kev/micron.

Instrumentation to measure the radiobiologically significant high-energy radiations encountered in manned spaceflight is of fundamental importance in ensuring astronaut safety and ultimate mission success. Since the discovery of the Van Allen Radiation Belts in 1958, and the advent of our knowledge of solar flare charged particles, it has been recognized that manned operations in near earth space would require a very careful consideration of these emissions. To date, manned space operations have not encountered dangerous radiation levels either because of the absence of high-energy solar flare particles, the avoidance of the highest fluxes of trapped particles in the earth's magnetosphere, or the relatively short duration of the missions where radiations were encountered. However, on future long-term missions the avoidance of such encounters will not always be possible and a very comprehensive measurement of radiation levels received by the crew must be realized. In this paper are described specially designed, active and passive dosimetry systems that will measure and record the radiobiologically significant radiations encountered in future manned spaceflight. Described specifically are instruments to be flown on the Skylab Programs, the first US. Space Station.

The most important radiations to be monitored in future extended long-term missions, like Skylab and the Orbital Space Stations, are solar flare, Van Allen Belt and primary cosmic protons with energies greater than 30 Mev. These particles exist in a complex and often unpredictable array of fluxes and spectra. For manned operations, the energy spectra and depositions of these particles must be measured at specific locations of astronaut activity.

Numerous ground-based experiments show that the degree of radiation effectiveness in impairing the functions of biological systems is determined principally by the two following parameters:

a. the locally absorbed radiation dosage,

b. the locally delivered linear energy transfer spectrum of the absorbed radiations (ref. 1).

The highly heterogeneous shielding afforded the astronauts by spacecraft and body self-shielding will cause high-energy protons to degrade in a very complex manner. This produces a significant depth dose gradient over the astronaut's whole body. The doses will also vary from astronaut to astronaut depending on shielding locations most frequented by him. Figure 1, after Schneider, (ref. 2) shows a measured variation of depth dose with shielding in the earth's inner Van Allen Belt measured on the Gemini 4 spacecraft.

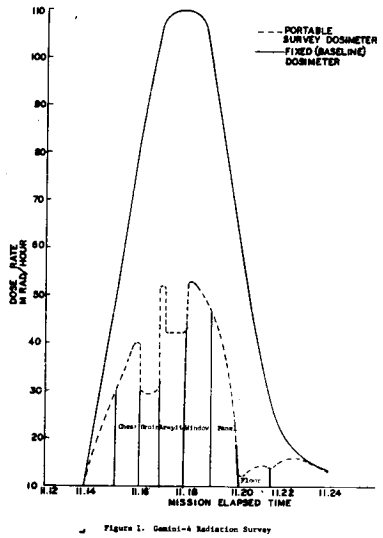

Figure 1. Gemini-4 Radiation Survey

An idealized picture of the theoretical depth dose behind 2.0 grams/cm^2 shielding for the Van Allen Belt and a typical relativistic solar flare as a function of a number of critical organ depths is shown in Figure 2 (Langham, ref. 3). It is emphasized that such depth dose gradients as these have not been measured for Skylab or the Apollo Command Module. Adequate space radiation dosimetry systems must lend themselves to the measurement of a large enough number of body points so that a depth dose gradient can be constructed. Also, dosimetry systems must record the average surface (skin) dose, and allow for the conduct of these measurements over short time periods to detect large changes in the radiation field. For example, on the Gemini flights the authors observed a rise of three orders of magnitude in the radiation levels in the spacecraft within a few minutes as the vehicles entered the Van Allen radiation belt.

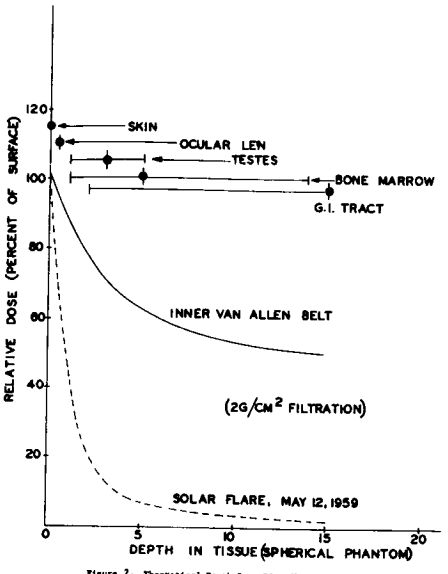

Figure 2. Theoretical Depth Dose Distribution for Critical Organs in Space Radiations

In order to indicate how the radiation dose is modified for radiations of different linear energy transfer, we examine Figure 3. Here, the variation of radiation RBE with LET values for mammalian tissues and crystalline lens cellular destruction and division is observed. We note also the recommended radiation protection values of relative biological effectiveness (RBE) as a function of LET, as defined by the 1967 United States National Radiation Protection Subcommittee, M-4 (ref. 4). There are wide variations in the RBE values for different radiation effects. For mammalian tissue damage the RBE is constant at a value of 1.0 for LET values of 3.5 kev/micron and less. The experimental RBE curve then shows a nonlinear rise to values of up to 5.0 for a LET of 100 kev/micron. The recommended RBE Subcommittee values of RBE vary from 1.0 at 3.5 kev/micron up to 20 at 100 kev/micron. The RBE Subcommittee established radiation protection values of RBE as a function of LET are generally higher and allow for larger safety factors than the observed experimental values.

The best use of the RBE-LET relationships is made by applying them to the various radiation effects on critical centers in the body such as the formation of cataracts in the eyes, gastrointestinal, skin and bone marrow damage, etc. As in the case of dose, this also requires measurement or simulated measurement of the LET at various depths. Especially important are measurements at depths where low-energy secondary radiations may significantly build up.

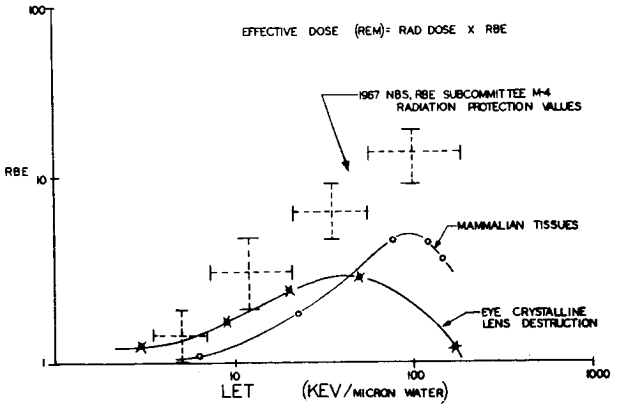

Figure 3. Effective Dose (REM) = Rad Dose X RBE

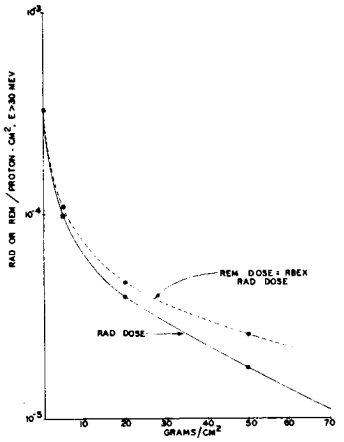

Figure 4. Calculated Rad and REM Dose as a Function of Shield Thickness for a Typical Inner Van Allen Belt Spectrum

For heterogeneous mixture of corpuscular radiations such as exist in the earth's radiation belts, in solar flares, and in galactic cosmic radiations, a wide spectrum of LET values may exist at various depths. The LET spectra must be measured and combined with the radiation surface doses and depth doses to give the REM dose.* The dose measurement problem in its most fundamental form reduces to one of determining the fraction of the dose (energy) delivered in each energy interval at the shielding depth of interest.

The LET spectrum in a spacecraft, such as Skylab, increases to higher dE/dX values as larger numbers of nuclear particles have their energy reduced closer to zero and as the number of secondary and recoil nuclei increases with increased shielding. The predicted effect of increased LET and RBE values with increasing shielding depth is clearly indicated in Figure 4 (Scott, ref. 5). Referring to this figure, the rem dose is calculated to increase to a factor of two over the rad dose at less than 50 grams/cm^2 of shielding, indicating that the LET values have increased greatly. This is a result of a wide variety of lower energy radiations, mostly secondary and degraded primary protons, secondary neutrons, and recoil nuclei produced in primary slowdown through heavier shielding. It is, therefore, important that the LET spectrum be determined where more than a first estimate of dose is required.

* REM Dose = RBE X Rad Dose. Where RBE is obtained from observed RBE versus LET relationships.

An adequate dosimetry system must be capable of conducting the following minimum measurements of the radiation field inside of the spacecraft:

a. the astronaut whole-body average surface dose levels,
b. the depth dose gradient at critical astronaut body organs (gastrointestinal tract, eyes, etc.),
c. the dose as a function of differently shielded spacecraft locations where the astronaut may be operating,
d. the instantaneous dose rates and depth dose rates delivered to the astronaut,
e. the accumulated or total mission doses and depth doses at the spacecraft shielding and body self-shielding locations previously mentioned,
f. the LET spectra at the same locations, where possible.

The above measurement must be conducted in the earth's Van Allen radiation belts and during irradiation from solar flare and primary cosmic charged particles, and from manmade trapped or onboard radiation sources.

Not only must an idealized dosimetry system be able to conduct these measurements, but it must also meet the criteria of small weight and size, be highly ruggedized, and have portable sensor elements. The systems must also have a wide radiation response range and excellent long-term accuracy. The radiation levels must further be determined where possible in a test material that has radiation reaction properties that closely match human

muscle tissue, i.e., the instrumentation must be able to measure the tissue equivalent dose levels from mixed radiation fields over an obviously wide range of energies. The active and passive dosimetry systems developed by the authors and described in the following sections of this report will be flown on the Skylab. They meet the above suggested criteria in the most accurate, reliable, and inexpensive manner currently possible with today's state of the art radiation detection methods.

Each active dosimeter system contains one tissue equivalent ionization sensor equipped for portable as well as fixed mounted operation combined in close proximity with a low energy charged particle spectrometer to measure LET spectra. With this instrument the astronaut can measure the dose, depth dose, and LET simultaneously and instantaneously inside a manned spacecraft. The radiation measurements are processed automatically by self-contained signal-conditioning electronic systems for recording by spacecraft telemetry.

Multisensor passive dosimeters at five (5) fixed mounted locations of minimum to maximum shielding have been developed and will be flown in the command module. Each passive dosimeter contains the latest state of the art ground based systems to measure total dose and LET spectra. The electronic and mechanical design of each subsystem is discussed in detail in the following sections. The spacecraft mounting locations of the active dosimeter and the five passive dosimeters are shown in Figure 5.

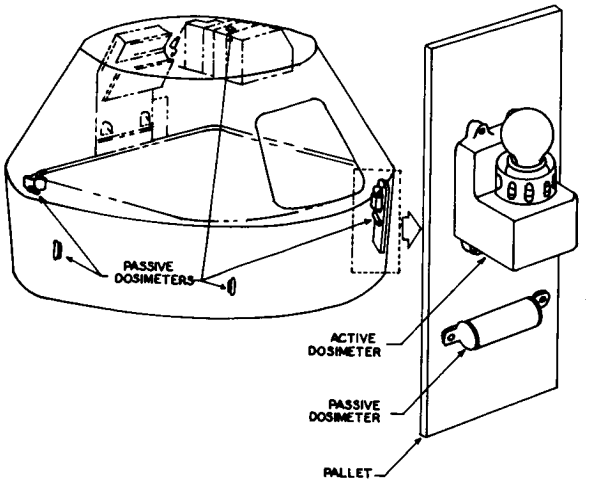

Figure 5. Active and Passive Dosimeter Locations in Command Module.

ACTIVE DOSIMETER SYSTEM DESCRIPTION

Tissue Equivalent Ionization Chamber System:

The active dosimeter described in this report involves the use of ionization chambers operated on the Bragg-Gray principle. This principle relates the ionization of a gas in a cavity contained in a medium to the absorbed dose in that medium. Ionization current in a gas cavity contained in a medium is related to the absorbed dose rate in the medium by the following linear equation:

$$E_m = S_m W J_{gas}$$

where: E_m = energy absorption in the medium in electron volts/gram sec

S_m = mass stopping power of the wall material relative to the gas

W = average energy in ev required to form

J_{gas} = ionization current in ion pairs/gram sec

According to Fano (ref. 6), if the gas and the surrounding medium in an ionization chamber are of identical atomic composition, the cavity may be large without disturbing the flux of secondary particles. More precisely this principle dictates that in a medium of given composition exposed to a uniform flux of primary radiation, the flux of secondary radiation is also uniform and independent of the density of the medium, as well as of the density variations from point to point.

The cavity ionization principle, therefore, permits a determination of energy absorption in a solid medium from the measured ionization in a small gas-filled cavity. This principle is the basis for the development of the advanced dosimetry system discussed in this report.

Since the biological damage resulting from ionizing radiation, in general, occurs in human tissue, the wall material of the ionization chamber that forms the medium in which the dose is measured should be tissue equivalent. The tissue usually chosen for this purpose is muscle tissue. The energy deposition is determined by the cross sections of each of the many chemical constituents making up tissue to the total radiation field encountered by that material. The cross sections are themselves dependent on the energy and type of radiation striking the tissue material. This means that the material of the ionization chamber walls must be as

closely matched in atomic composition to the atomic composition of human muscle tissue for the chamber to be tissue equivalent to the particle flux entering the spacecraft. That is, the material making up the walls should have cross sections and stopping powers for all possible encounterable radiation that are very closely matched to standard muscle tissue. Shonka (ref. 7) has developed a series of plastic resins that are ideally suited for this purpose. These are the plastics that were chosen for the Skylab Ionization chamber sensors. A comparison of Shonka plastic to the standard muscle composition as defined by the International Committee of Radiological Units ICRU (ref. 8) is shown in Table I. To avoid the necessity for making energy dependence corrections to the dose, it is measured directly in our dosimetry system by using Shonka sensor material previously described. This allows an unperturbed tissue response to be realized at all points of interest for all possible radiations. Fano's principle requires that to have an ionization chamber cavity of reasonably large volume capable of measuring the dose in a tissue equivalent medium, the gas should be matched atomically to this medium. A suitable nonexplosive tissue equivalent gas comprising methane, carbon dioxide, and nitrogen in the proportions shown in Table II is employed inside the chamber.

Table I

ICRU MUSCLE COMPOUND AND SHONKA CHEMICAL COMPOSITION

Element	Atomic Number	ICRU Muscle Percent by Weight	Shonka Plastic Percent by Weight
H	1	10.20	10.25
C	6	12.30	76.05
N	7	3.50	3.50
O	8	72.90	5.19
Na	11	0.08	0.08
Mg	12	0.02	0.02
P	15	0.20	0.20
S	16	0.50	0.50
K	19	0.30	0.30
Ca	20	0.007	0.007

Table II

TISSUE EQUIVALENT GAS COMPOSITION

Element	Composition by Weight (percent)
C	45.6
O	40.8
H	10.1
N	3.5

Observations of the gamma and neutron sensitivity of a tissue equivalent ionization chamber using this filling gas have indicated that it is stable to $\pm$ two percent over a nine month period; demonstrating that negligible changes in the filling gas occur through diffusion or absorption losses in the cavity wall during the period of measurement. Since the relative mass stopping power of the wall to gas is unity, the Bragg-Gray relation reduces to $E = WJ_{gas}$.

The radiation produced ionization chamber current is conditioned by the following electrical subsystems which comprise the complete tissue equivalent ionization chamber system. These systems are manufactured in a flight-ready configuration by the AVCO Electronics Division/Tulsa.

a. Sensor and Preamplifier
b. Operational (Signal Conditioning) Amplifier
c. Power Supply
d. Temperature Monitor

The tissue equivalent ionization chamber sensor consists of two electrodes. One is an 0.0625-inch-thick Shonka Type A-150 tissue equivalent plastic sphere described previously with an inner diameter of 2.188 inches. This spherical shell acts as the high voltage electrode for the ionization chamber system. The other ionization collecting electrode is a thin cylindrical probe 0.05 inch in diameter and 0.747 inch long centered within the spherical outer electrode. The collecting electrode is connected directly to the grid of a Raytheon CK 8520 electrometer. The CK 8520 preamplifier, Figure 6, collects and amplifies the instantaneous ionization current formed in the tissue equivalent cavity

operates in the triode connected floating grid mode. Experiments show that the triode connected electrometer has the following relationship between the grid and plate currents.

$$i_p = (s \log_{10} i_g + q)^{3/2}$$

where: i_p = the plate current

i_g = the grid current

s = a proportionality constant dependent on the cathode temperature and the tube geometry

q = dependence of plate current on current on cathode temperature, the tube geometry, the grid to cathode potential, the plate voltage, and amplification factor (which is in turn dependent on the tube geometry).

For an optimum filament current of 10 milliamperes at 1.50 volts and a plate voltage of 6.5 volts, the above relationship for an 8520 electrometer has the following form:

$$i_p = (4.43 \log_{10} i_g + 94.5)^{3/2}$$

The plate current of an 8520 electrometer varies with the log of the grid current over eight decades or orders of magnitude of the grid current. Thus, this system can be used to measure radiation induced currents from 5.0×10^{-15} amperes to over 10^{-7} amperes. This wide range of current values allows for the measurement of all known levels of ionization resulting from cosmic rays, solar flare particles, or the trapped Van Allen particles that might be encountered on manned space missions.

The plate current, which is typically several hundred microamperes in magnitude, is input for the final signal conditioning amplifier that connects with the spacecraft telemetry system.

The signal-conditioning amplifier displayed connected with the sensor and preamplifier is shown in Figure 7. The signal conditioning amplifier subsystem changes the CK 8520 electrometer plate current (typically a few hundred microamperes) to a 0.0 to 5.0 volt dc level compatible with spacecraft telemetry. It is a Fairchild SN 52709 high-gain operational amplifier constructed on a single-silicon chip using special planar epitaxial processes. It features high-input impedance, low offset, large input common mode range, and high output swing under load. The system is a low power device drawing less than 300 milliwatts maximum power and less than 150 milliwatts as operated in the tissue equivalent ionization chamber system. Additionally, the operational amplifier is highly stable with temperature over the range -55°C to 125°C, as a result of excellent internal temperature compensation.

The signal conditioning subsystem is designed with both gain and bias adjustments. These adjustments are used to set the dc level and slope of the input current versus output voltage curves before flight of the instrument.

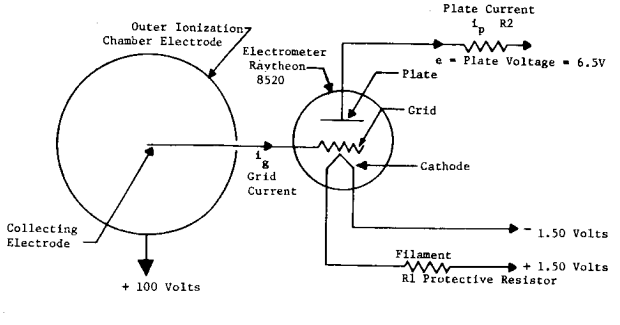

Figure 6. Tissue Equivalent Ionization Chamber Sensor and Preamplifier

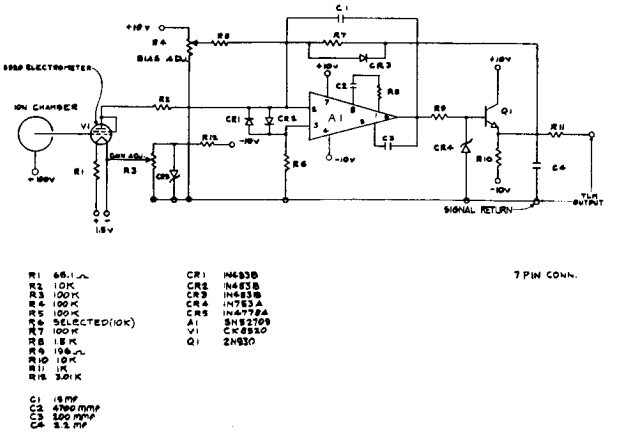

Figure 7. Tissue Equivalent Ionization Chamber Sensor, Preamplifier and Amplifier

The electronic conversation unit (power supply) subsystem for the TEIC is a standard dc to dc converter with series input regulation and hard diode protection. The dc to dc converter supplies high voltage for the ionization chamber high-voltage electrode, electrometer plate and filament voltages, and the driving voltages for the signal conditional amplifier and temperature sensor.

The flight configuration of the tissue equivalent ionization chamber sensor, Figure 8, is constructed of three walls. The inner wall consists of the high-voltage, tissue-equivalent Shonka plastic 2.31-inch outer diameter sphere covered with a second wall of 0.0625-inch thick epoxy coating to electrically isolate the inner conductive sphere from the third or outer wall. The outer wall is the hermetic seal for the two inner walls. It consists of a 0.025 $\pm$ 0.005-inch thick aluminum sphere. These three concentric spheres are attached to a cylindrical (also triple walled) barrel assembly housing the inner collecting electrode and the Raytheon CK 8520 preamplifier electrometer. The outer aluminum housing for the cylindrical barrel is machined in a single assembly with one of the hemispheres of the sensor. This assembly is hermetically sealed by press fit arrangement at the hemispherical interface shown in Figure 8.

The tissue equivalent ionization chamber electronic subsystems exclusive of sensor and preamplifier are packaged in hermetically sealed steel containers. The signal conditioning amplifier and temperature sensor subsystems are packaged in one container and the power supply is housed in the other container. Electrical interconnections between modules are made with special teflon insulated wire approved for flight on the Skylab Program.

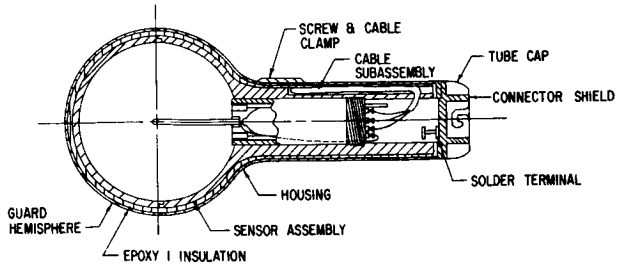

Figure 8. Multiple Wall Sensor Assembly

LINEAR ENERGY TRANSFER (LET) SPECTROMETER SYSTEM DESCRIPTION

The linear energy transfer (LET) spectra of space radiations are in general extremely complicated and difficult to measure activity. This is evidenced by the previous lack of such devices on manned spacecraft. Sensors have been developed in ground-based experiments (Rossi, ref. 9) to measure the LET spectrum employing low-pressure proportional counters. The Air Force Weapons Laboratory designed and tested similar types of space hardened gaseous proportional counters for use on satellite flights and high altitude aircraft flights to measure the anticipated LET spectra encountered in spaceflight. Instruments of this type have, however, had only very limited success in spaceflight. Limitations were due to problems involved with maintaining stable gas pressures and compositions in the low-pressure environment of space for extended periods and the poor resolution of such devices. The numerous difficulties encountered by attempts to use proportional counters in space to measure the LET spectrum are avoided on Skylab by the use of solid state semiconductor detectors. These devices are commercially available in long life, high reliability versions that can be obtained in almost any variety of detector thickness.

The LET spectrum for radiation penetrating the wall of the spacecraft indicates the quality or the relative biological effectiveness (RBE) of the radiation. The lower energy protons have high LET and a correspondingly high RBE. For example, protons of energies less than 14 Mev have LET greater than 3.5 kev/micron in water or muscle, and RBE greater than 1. Assuming 2 gm/cm^2 aluminum as representative of the spacecraft wall thickness at which the active dosimeter will be mounted and tested, trapped protons having external energies $40 < E < 46$ Mev are those which will have energies < 18 Mev inside the spacecraft. These are most easily measured by determining their total energy deposition in the solid state detectors. The same detectors can also measure alpha particles up to 75 Mev entering the spacecraft. The proton and alpha particle counts and energies measured by the method of total energy deposition are coverted to LET spectra using range, energy, and (dE/dX = LET) tables generated by the author, Janni (ref. 10). The relative $\frac{dE}{dX}$ versus E

responses for silicon and standard muscle tissue are uniquely defined and are shown in Figure 9. The $\frac{dE}{dX}$ values for the two materials are related by a well known mathematical function over the energy range which will make conversion from $\frac{dE}{dX}$ in silicon to muscle a straightforward process. The total counts in the intervals 0.5 to 18.5 Mev and greater than 18.5 Mev are also normalized for the tissue equivalent ionization chamber dose rate readings for baseline data in the depth dose radiation surveys with the portable tissue equivalent ionization chamber.

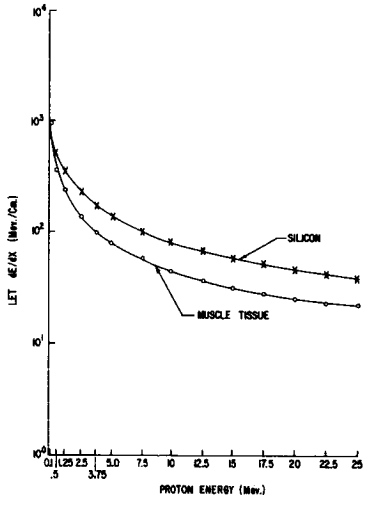

Figure 9. Stopping Power as a Function of Proton Energy

The LET system described in this report consists of two lithium drifted silicon solid state detectors operated as a charged particle telescope in near proximity to the tissue equivalent ionization chamber to record and to measure the energy of protons and alpha particles entering the spacecraft. The LET detectors designed by the authors are manufactured by Nuclear Semiconductors Inc. The first (entrance) solid state detector shown in Figure 10 is 2000 microns thick to provide the desired energy analysis of the high linear energy transfer components (lower) proton and alpha particle energies of the radiation environment entering the spacecraft. The second or anticoincident detector is 1000 microns thick. These two detectors are shielded with tungsten such that the protons and alpha particles enter them almost entirely from one plane so that they can be analyzed. The 2000-micron detector of the charged particle telescope measures the proton energies between 0.5 Mev and 18.5 Mev in five energy increments: 0.5 to 2.0, 2.0 to 6.0, 6.0 to 10.0, 10.0 to 14.0, and 14.0 to 18.5; and alpha particles between 18.5 and 75 Mev. The corresponding LET ranges are protons: 16 to 42.4 kev/micron, 6.8 to 16 kev/micron, 4.5 to 6.8 kev/micron, 3.5 to 4.5 kev/micron, 2.8 to 3.5 kev/micron, and < 2.8 kev/micron alpha particles: 10.4 to 32 kev/micron.

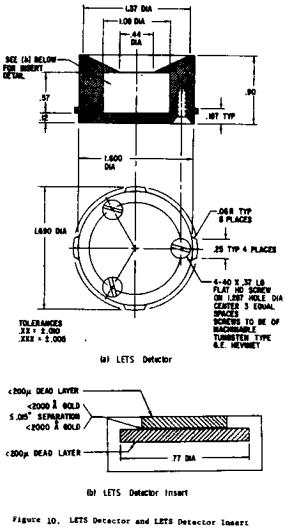

(a) LETS Detector

(b) LETS Detector Insert

Figure 10. LETS Detector and LETS Detector Insert

Original design plans for this system called for a four detector type telescope consisting of an additional thin (less than 20 microns) planar solid state detector and an annular solid state detector in the telescope arrangement shown in Figure 11. The four-detector system would extend energy measurements down to 0.1 Mev for protons and would expand the range of proton LET measurements to 93 kev/micron. Additional high LET multicharged particle measurements resulting from cosmic rays and recoil particles are readily possible with this larger system. The electronic block diagram for the four-detector system is shown in Figure 12. The basic electronic subsystems for the four-detector arrangement are analagous to those described later for the two-detector LET system. This system will not be flown because of telemetry and manufacturing cost constraints. Instead the two-detector LET system will be employed in the Skylab active dosimeter.

The LET electronics to shape, analyze, select, and telemetry condition the charged particle pulses produced in the solid state detectors, are displayed in block form in Figure 13. These are as follows:

a. Detectors, preamplifier, shaper, and voltage amplifiers
b. Analyzer buffer amplifiers
c. Analyzers (Discriminators)
d. Analyzer logic
e. Delayed strobe
f. MOSFET counters (seven-bit stair steps)
g. Ratemeter
h. Telemetry buffer amplifiers
i. Power supply

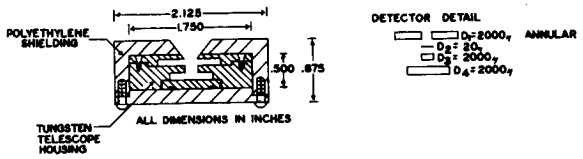

FOUR DETECTOR SOLID STATE LET TELESCOPE

Figure 11.

4 DETECTOR SOLID STATE LINEAR ENERGY TRANSFER (LET) SYSTEM

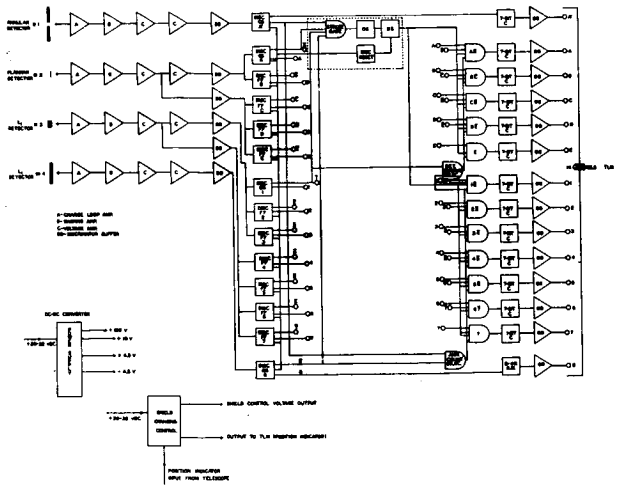

Figure 12.

The charge signals originating in the solid state detectors are converted to voltage signals by special charge loop preamplifiers A1 (see Figure 13). These amplifiers have a sensitivity of approximately 10 millivolts/Mev of energy loss in the silicon solid state detectors. The voltage pulses from the charge loops are processed by the shaper amplifiers A2 shown in the same figure. This amplifier develops a gain of 10 and has 0.5 x 10^{-6} second equal integration and differentiation. The signal is finally amplified by specially designed X10 voltage amplifiers A3.

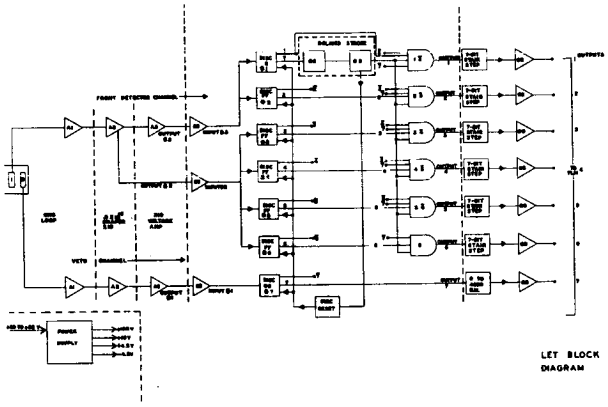

Figure 13.

The detailed electrical schematics for the detectors, preamplifiers, shaper amplifiers, and voltage amplifiers are shown in Figure 14.

The pulse height analyzers (discriminators) select the shape and amplified voltage pulses according to their amplitude into distinct energy channels. The pulse height analyzers are integrated circuits, RCA type CD2203s. Electrical schematics of the discriminators are displayed in Figure 15.

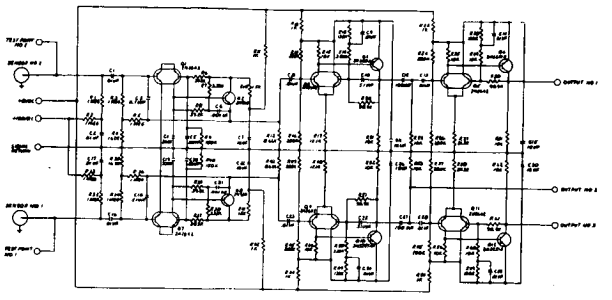

Figure 14. Schematic Detectors and Preamplifiers

Integrated circuits A8 and A9 comprise the delayed strobe shown in Figure 15. A9 generates pulse inversion for the delayed strobe while A8 is a double one-shot (the first one-shot has a 3 microsecond delay and the second has a 7 microsecond delay). This pulse action by the delayed strobe resets the discriminators and logic circuitry of the LET system so that they are in the ready-to-count condition. Since count rates of the order of no greater than 200 per second on the Skylab mission are anticipated, this is satisfactory.

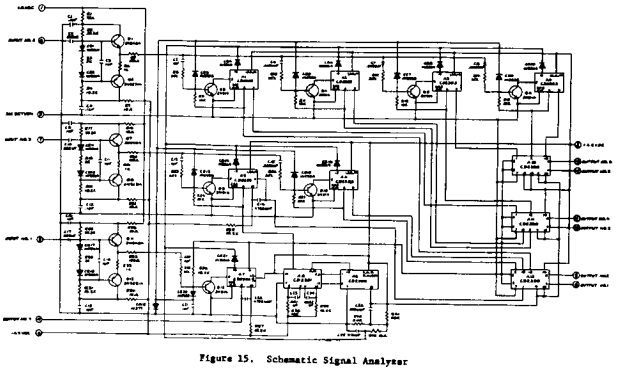

Figure 15. Schematic Signal Analyzer

The MOSFET (Metal Oxide Silicon Field Effect Transistor) counters are shown in Figure 16. They are RCA CD4004T MOSFET counters in ladder adder R-2R networks. These counters are output for the six energy analyses channels of LET detector.

The ratemeter for the LET system in Figure 16. is the output of the anticoincidence (second) detector. It transfers particle count rate received into a steady 0.0 to 5.0 volt dc level. It is the only nonlinear ramp type output that the LET system has. The ratemeter is a semilogarithmic device that is set so that 0.0 to 4000 counts/minute are recorded on a 0.0 to 5.0 vdc scale.

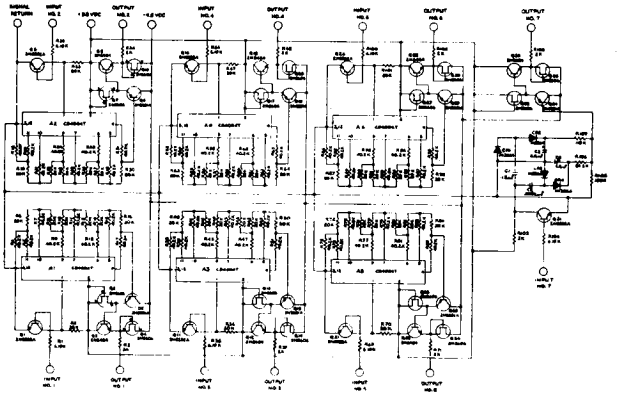

Figure 16. Schematic Counter and Output

The LET power supply system in Figure 17. supplies voltages to operate all other electronic subsystems just described. The power supply is designed to operate from a dc input of 28 + 4 or -8 volts of unregulated spacecraft power.

The power supply regulator is the integrated circuit component A1, a National Semiconductor LM100 transistor.

The LET electronics described in this report are packaged in four separate module subsystems. Each module corresponds to one of the major electronic systems and is hermetically sealed in steel cannisters of the same type of design as those used in the tissue equivalent ionization chamber electronics.

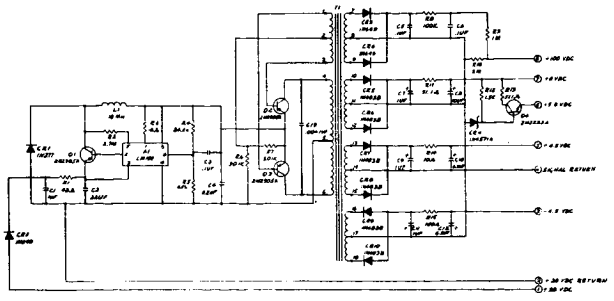

Figure 17. Schematic, Power Supply

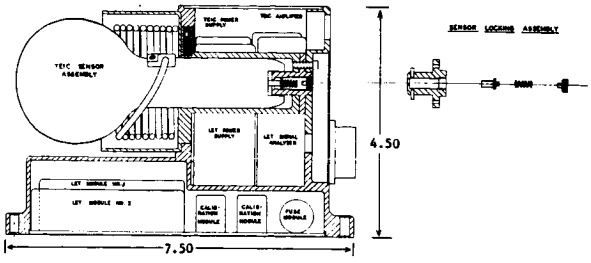

Figure 19. Active Dosimeter Module Mounting Sensor Locking Assembly Side Views

The tissue equivalent ionization chamber and LET electronics are mounted into a single, small 135 in^3 package with modules shown in Figures 18 and 19. The tissue equivalent ionization chamber is locked into the mounting case but can be removed to a length of over 6.5 feet for cabin and astronaut on-body surveys. During the Skylab mission fourteen (14) selected astronaut on-body and spacecraft shielding locations will be surveyed by the crew for Van Allen Belt, and cosmic ray encounters. The LET detector total counts will be normalized to a fixed location dose as base line date during the surveys.

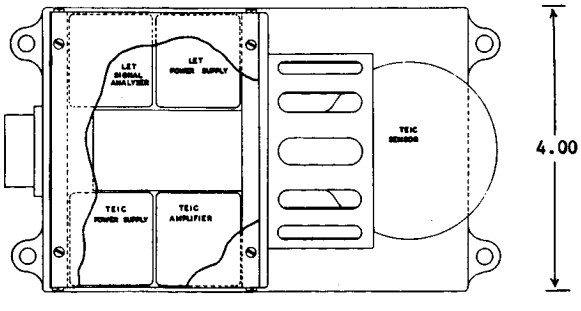

Figure 18. Active Dosimeter Module Mounting - Top View

The Skylab active dosimeter has nine electrical output signals.

The following description of each output channel, parameter sampled and sample rate is given:

Channel	Parameter Samples	Sample Rate
$TEIC_1$	TEIC dose rate	every 0.8 sec
LET_2	Proton energy, ΔE_1	every 0.8 sec
LET_3	Proton energy, ΔE_2	every 0.8 sec
LET_4	Proton energy, ΔE_3	every 0.8 sec
LET_5	Proton energy, ΔE_4	every 0.8 sec
LET_6	Proton energy, ΔE_5	every 0.8 sec
LET_7	Proton anticoincidence	every 0.8 sec
LET_8	Alpha particle count	every 0.8 sec
$TEIC_9$	Temperature sensor	every minute

The output impedences of each of these channels ranges between 2000 and 5000 ohms for compatibility with a greater than 1-megohm spacecraft telemetry.

The nine data outputs of the active dosimeter are decommutated after transmission from the spacecraft commutator to ground and placed on magnetic tape as a function of time. The data are in 550 bits per inch BCD format. The telemetry output voltage cannot exceed +5.0 VDC nor drop to less than -0.5 VDC. Continuous coverage is also employed where possible. When full coverage by ground stations is not possible, the output can be stored on an on-board tape recorder and relayed as soon as possible thereafter to ground facilities. The use of an on-board tape recorder having a data storage capacity of 90 minutes is used for full coverage in a 200-mile orbit around the earth. The data for an entire revolution are then dumped to one ground

station and placed on one tape. The resulting data are continuous in time. This greatly simplifies data processing.

ACTIVE DOSIMETER PERFORMANCE AND TEST DATA

The tissue-equivalent ionization chambers are calibrated with gamma radiations from the isotopes of Cobalt-60 and Cesium-137. Calibration is conducted on NBS certified radiation ranges to ensure the radiation response of the instruments. The radiation response as a function of output voltage is displayed in Figure 20. The radiation range is 0.2 millirad/hr to 25 rad/hr using an 0.0 to 5.0 volt telemetry range. It is possible by expanding the telemetry range to measure dose rates of 10^3 rad/hr. The response times of the tissue-equivalent ionization chambers are determined by timing their performance under irradiation by the sources described above. The following response time data have been generated for the tissue equivalent ionization chamber.

Radiation Level	Rise Time (sec)	Decay Time (sec)
2.9 mrad/hr to 1.05 rad/hr	0.525	1.40
10.0 mrad/hr to 5.7 rad/hr	0.480	1.50
0.5 rad/hr to 16.5 rad/hr	0.21	.45

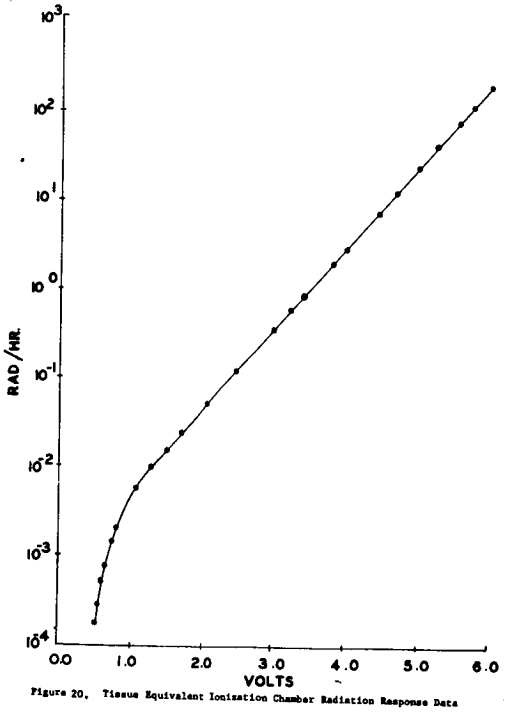

Figure 20. Tissue Equivalent Ionization Chamber Radiation Response Data

The rise time is defined as 90 percent of the lowest radiation value indicated, and the fall time is 110 percent of the lowest radiation level. The instrument is stable with temperatures between 0° and 120°F. For temperatures between -40° to 160°F, the instrument will not drift by more than 5 percent from its radiation response at room temperature.

Three types of tests are employed in calibrating the LET system. These are:

a. radiation sources
b. precision pulser
c. cyclotron irradiation

Americium-241 alpha particles of energy 5.476 Mev are used to activate the first two LET data channels 0.5 to 2.5 and 2.5 to 6.0 Mev. The alpha source cannot be employed after final assembly of this system because the entire LET is hermetically sealed. Therefore, functional and prelaunch testing is conducted with strontium-90 beta rays.

A precision 1 micro-micro farad capacitor is mounted to each input of the preamplifiers to conduct tests with an electronic pulser. The capacitors are mounted to the first input pin of the preamplifier. The capacitors are connected through a coaxial cable system to pins in the system's power and signal connector. Pulses from a precision pulser are applied to the preamplifier inputs. The test pulse has a rise time of approximately 10^{-8} seconds and a decay time of about 3×10^{-4} seconds. Each solid state detector produces approximately 4.5×10^{-4} coulombs of charge for each Mev liberated in it. Using the simple relation $V = Q/C$ the pulse amplitude X, that is equal 45 millivolts. This is easily measurable. Pulses equivalent to 1.5, 4.0, 7.5, 12, 15, and 50 Mev are used to test the six LET channels.

Measurements have been conducted at the Texas A&M University and Oak Ridge National Laboratory cyclotrons using degraded proton beams to ensure that the proper energy detection and pulse discrimination were achieved by the LET electronics. The results of these irradiations with protons of 60, 30, 25, 20, 15, 12, 9, and 5 Mev indicated satisfactory operation of the LET's system. The LET electronics system is insensitive to within 1% for temperatures between -40°F and +160°F.

PASSIVE DOSIMETRY SYSTEMS

The passive dosimetry portion of the Skylab radiation monitoring systems determine the radiation intensities at five fixed shielding locations within the Apollo command module, and seven similar locations in the Orbital Workshop. These intensities will be a function of the space radiation environment exterior to the spacecraft, mission length, orbital variables, and dosimeter location within the command module. The passive dosimetry units will be located at points approximating maximum, minimum, and intermediate shielding each containing the following dosimeters: lithium fluoride and calcium fluoride thermoluminescent dosimeters, a quartz fiber ionization chamber, nuclear emulsions, plastic polymers, and gold and iridium foils. The individual components making up each Skylab passive dosimeter unit are discussed in the following paragraphs.

Each dosimeter unit for Skylab includes a series of small rugged individual dosimeters housed in a sealed aluminum cannister. A diagram of the aluminum mounting containers and each of the individual dosimeters within the small cylindrical container are shown in Figure 21. Figure 22 shows the aluminum cannister construction teflon shock mounts, and the mounting arrangement of the individual dosimeters. The cannister and the end mounts are anodized aluminum. The O-ring is circular in shape and is constructed of Teflon. Since the passive dosimeters do not require any electrical power or telemetry connections there are no electrical plugs or feed-throughs.

Several types of radiation detectors are housed within the aluminum container. The selection of the dosimeter material was strongly influenced by the volume and weight limitations which are associated with spaceflight. Each passive dosimetry unit, including all contents and the aluminum container, will weigh only 0.37 pounds. The weight restrictions do not allow the more standard technique of successively varied and increased shield thickness about each dosimeter to be used. For this reason, the inherent charged particle response of the various individual dosimeters will be used to evaluate the particle type and energy cut-off. Only one clacium fluoride thermoluminescent dosimeter will be shielded. The dosimeters selected for use are each discussed in the following paragraphs.

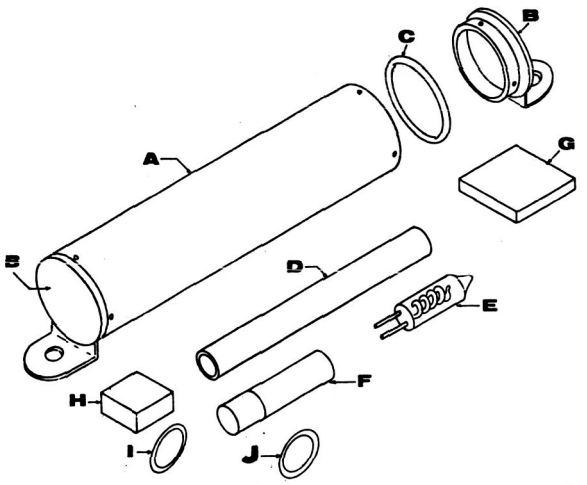

FIGURE 21 Complete Dosimeter Unit (Graphic Anatomy)

A. Aluminum Dosimeter Unit Housing
B. Aluminum Dosimeter Unit Housing End Plate
C. Teflon Seal
D. Ionization Chamber, Pocket Dosimeter
E. Thermoluminescent Dosimeter
F. Thermoluminescent Dosimeter Shield
G. Polymer Dosimeter
H. Nuclear Emulsion Dosimeters (Types K-2 and G-5)
I. Gold Foil
J. Iridium Foil

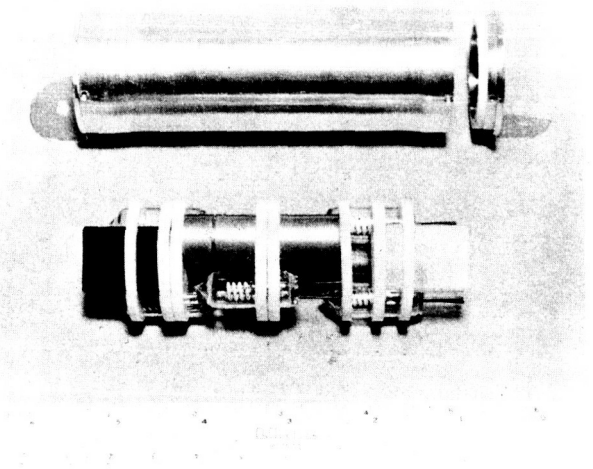

Figure 22. Passive Dosimeter Container Showing Mounting Locations of Individual Sensor Elements.

Thermoluminescent Dosimeters:

Several types of thermoluminescent dosimeters are commercially available, but only the glass enclosed lithium fluoride and calcium fluoride types manufactured by EGG (Durkee, ref. 11) are used. When a thermoluminescent material is irradiated, electrons become trapped at lattice imperfections within the crystalline solid. This trapping is relatively stable at temperatures on the order of 70°F, but the addition of large amounts of thermal energy causes the electrons which were trapped within the imperfections of the solid to be thermally agitated, allowing them to combine with charge carriers of the opposite sign. Visible light is emitted in this process which can be correlated with the amount of absorbed energy that has been deposited within the material. Calcium fluoride and two isotopes of lithium fluoride will be flown in the Skylab passive dosimeter systems. These materials are evenly coated on a heating element sealed within a glass container similar in construction to a small vacuum tube. The coating of the powder on an ohmic heater allows a known quantity of heat to be applied to this powder, and also provides a very high degree of reproducibility in the system. The powder must be heated in a vacuum or a pure inert gas atmosphere to eliminate spurious luminescence peaks which would otherwise occur. The vacuum technique also eliminates errors caused by inaccurate weighing, chemical change, or handling. The emitted light is blue-green and is measured post flight by using a photomultiplier tube and an associated electronics system to determine the intensity of the light emission. This dosimetry system is quite sensitive and can record total doses as low as 10 millirads approaching accuracies of 10 percent. The percent accuracy improves rapidly as the total dose increases and is about 5 per percent at 50 millirads. A shield will be used on one of these dosimeters in each cannister to provide charged particle cut-off points at reasonably well defined energies.

Two different lithium isotopes will be used to determine the contribution of secondary thermal neutrons to the total dose. Because the Li^6 isotope has a very low neutron cross section, the difference between the readings of the Li^6 and Li^7 types of lithium fluoride is interpreted as the thermal neutron dose. The Edgerton, Germeshausen, and Grier thermoluminescent dosimeters and associated shields will be used, and have the following common designation: lithium fluoride dosimeter - EGG TL-12, calcium fluoride dosimeter - EGG TL-21, and shield - EGG TL-32.

Nuclear Emulsions:

Practical methods of obtaining comprehensive information on the Linear Energy Transfer (LET) using passive dosimeters are limited to the use of nuclear emulsions. The most severe problem associated with the use of emulsions on long duration missions is that of track fading with time. A variety of emulsions are available and some have more severe fading characteristics than others. Emulsions of the Ilford G-5 and K-2 types are very suitable and have been chosen for use on Skylab. The dose fading is considerably less for the G-5 emulsion than for the K-2 types. However, this fading will not introduce particle losses greater than 30 percent for missions of one month.

The G-5 emulsion is considerably more sensitive than the K-2 emulsion. Using a combination of these two emulsions allows resolution of proton and alpha tracks of low energies which would be saturated in the G-5 emulsion alone but which still may be cleanly detected in the K-2 emulsion. This arrangement also allows discrimination of electrons from protons and alphas over the LET range 0.2 kev/micron to >85 kev/micron. This is accomplished by post flight microscopic examination of the individual particle tracks in the developed emulsions. The track count and grain density are then used to establish the atomic number of the charged particle, and the straggling and scattering of the tracks may be used to differentiate electrons from the heavier protons and alphas.

After a statistically significant number of particle tracks have been counted over a broad range of energy deposition values, an integral spectrum can be determined. This is then differentiated to obtain a differential spectrum. The tissue dose is required for comparison with active dosimeter data. The tissue dose is established by assuming the track population in the emulsion is the same as would have existed in an equivalent volume of tissue.

The tracks from protons and helium nuclei are very similar and the majority cannot be distinguished. However, a differential LET distribution for these Particles can be determined, and the tissue dose can still be found. The tissue-equivalency problems associated with the use of these emulsions are circumvented in this manner.

A large amount of bremsstrahlung would register in the emulsions as an increased electron population. The greater majority of such secondary electrons are readily identifiable.

Emulsions which have grains and grain spacing much larger than nuclear track emulsions are not capable of producing individual tracks. An increase in the optical density as a function of incident radiation intensity for those types of emulsions allows them to be used as dosimeters. Although this method has been widely used in health physics applications, there are still calibration and processing uncertainties as well as serious tissue equivalency problems with the use of such emulsions in unknown radiation fields. Because the LET cannot be determined, densitometric emulsions cannot be directly corrected to tissue response as can nuclear track emulsions. For these reasons, densitrometric emulsions are not included in the Skylab passive dosimeters, and only the Ilford G-5 and K-2 nuclear track emulsions will be used. The nuclear emulsions will be processed and analyzed for the authors by Dr. Herman J. Schaefer of the Naval School of Aviation Medicine.

Plastic Polymers:

Several plastic polymers are capable of recording the heavy ion component of the galactic cosmic radiation. These detectors have a number of characteristics that make them particularly appropriate for this application. They are light, rugged, compact, insensitive to temperature and humidity changes, have no latent image fading at ordinary temperatures, and are straightforward to process. Since protons and electrons are not registered, the heavy ions can be detected without being masked by an associated proton or electron population. This method allows classification of multicharged particles by their rate of energy loss.

The polymers as flown on Skylab consist of a sandwich of three layers of different polymers, each having a well-defined sensitivity. A particle traversing this system will leave tracks in some polymers and not in others. Counting tracks in each of the polymers gives the flux of particles above some known value of LET. By subtracting the fluxes recorded in adjacent materials, the flux of particles in a given broad range of LET can be obtained. The resolution of such a system depends upon the number of polymers used, and at least three polymers are required to provide adequate information concerning the heavy particle contribution for mission radiation.

Activation Foils:

Dosimetry by means of activation foils suffers from two primary difficulties. First, activation foils are relatively insensitive to radiations of low level and are not capable of measuring low doses; and second, the information contained in an activation foil decays away with the passage of time. Nevertheless, two types of activation foils are suitable for use in the Skylab passive dosimeter units to provide an evaluation of the neutron fluences. These are small gold and iridium foils which are being included because of their very low volume and weight.

A small gold activation foil will be used to provide information concerning the thermal neutron detector having an effective cross section of 98.9 barns with a half life of 2.7 days (Murphy, ref. 13). The large cross section tends to offset the radioactive decay resulting from the 2.7-day half life. The thermal neutron detectability within one half life is about $10^6 n/cm^2$. Except for the resonance at 5 ev, gold is not an epithermal or high energy neutron detector. With modern counting equipment and proper care, gold activation equivalent to one rad of thermal neutron fluence can still be counted after 10 half lives.

Iridium is the second activation foil which will be used and is sensitive over a broader neutron energy band than gold. Two isotopes of iridium will be used to detect thermal as well as higher energy neutrons; both isotopes will be contained within the same foil. The $_{77}Ir^{191}$ isotope is 38.15 percent abundant and under neutron irradiation goes to $_{77}Ir^{192}$ via two metastable states. The $_{77}Ir^{193}$ isotope is 61.5 percent abundant and has a neutron capture cross section of 110 barns; the product nucleus is $_{77}Ir^{194}$. The effective

neutron capture cross section for naturally occurring iridium containing both the $_{77}Ir^{191}$ and $_{77}Ir^{193}$ isotopes is 453 barns, with 385 barns (Lederer, ref. 13) being contributed by the 38.5 percent abundant $_{77}Ir^{191}$.

Other types of activation foils are not being included in the passive dosimetry experiment because their combination of half life and neutron cross section make them unsuitable.

Quartz-fiber Ionization Chamber:

Operation of the quartz-fiber dosimeters is well known. They consist of a sensitive chamber, a quartz-fiber electrometer, and a charging system. This response time is determined by the capacitance between the various parts of the chamber.

Response times of dosimeters of this type are generally quite rapid and are more than adequate to record the slowly accumulating dose anticipated on the Skylab mission. Dose fading is usually not negligible in such dosimeters and may be as large as 1 percent per day; however, the dosimeters selected for this flight are manufactured by the Dosimeter Corporation, Cincinnati, Ohio, and have leakages much less than this.

Analysis Considerations:

In order that the passive dosimeters record primarily the radiation dose during the length of the flight, and not the background accumulation which is caused by the galactic cosmic radiation which penetrates to the Earth's surface, the flight passive dosimeters will be installed in the spacecraft three days prior to launch. The standard use of ground control dosimeters configured identically to the flight units will be used. The flight dosimeters will be recovered as soon as possible after splashdown and returned to the AFWL for analysis. Prompt recovery is important because of the dose fading characteristics of several of the individual dosimeters. Recovery within two days after splashdown is programmed.

REFERENCES

1. Janni, J. F. and Holly, F. E.; Chapter IV "Space Radiation Dosimetry" Aerospace Medicine Vol 40, No. 12, December 1969, pp 1462-1475.

2. Schneider, M. R., and Janni, J. F.; "Experiment D-8, Radiation in Spacecraft, Gemini-4," First Manned Spaceflight Symposium, p 171, Wash DC, 1965.

3. Langham, W., Chapter III, "Biological Effects of Ionizing Radiation," Aerospace Medicine, Vol 36, No. 2, p 32, 1965.

4. United States National Radiation Protection Subcommittee, M-4 Report, 1967.

5. Scott, W. W.; Estimates of Primary and Secondary Particle Doses Behind Aluminum and Polyethylene Slabs Due to Incident Solar Flare and Van Allen Belt Protons, RSIC-18, Oak Ridge National Laboratory, Tennessee, July 1967.

6. Fano, U., Radiation Research, Vol I, p 237, 1954.

7. Shonka, F. R., et al; Proceedings of the Second United Nations International Conference on the Peaceful Uses of Atomic Energy, 21, p 184, 1958.

8. "Report of the International Commission on Radiological Units and Measurements (ICRU)," National Bureau of Standards Handbook 78, 1959.

9. Rossi, H. H., and Rosenzweig, O.; Radiology, 64, No. 3, pp 290-299, March 1955.

10. Janni, J. F., Calculations of Energy Loss, Range, Pathlength Straggling, Multiple Scattering, and the Probability of Inelastic Nuclear Collisions for 0.1 to 1000 Mev Protons, AFWL TR-65-150, Air Force Weapons Laboratory, Kirtland AFB, New Mexico, September 1966.

11. Durkee, R. K., et al; Energy and Rate Dependence Studies, EG&G Technical Report S-237-R.

12. Murphy, H. M., Summary of Neutron and Gamma Dosimetry Techniques, AFWL Technical Report AFWL TR-66-111 (1967).

13. Lederer, C. M., Holtauclen, J. M., Perlman, I.; Table of Isotopes (Sixth Edition), John Wiley & Sons, Inc., New York (1967).